Operational Space Technology for Global Vegetation Assessment

Felix N. Kogan
National Oceanic and Atmospheric Administration/National Environmental Satellite, Data, and Information Services, Camp Springs, Maryland

ABSTRACT

The main goal of global agriculture and the grain sector is to feed 6 billion people. Frequent droughts causing grain shortages, economic disturbances, famine, and losses of life limit the ability to fulfill this goal. To mitigate drought consequences requires a sound early warning system. The National Oceanic and Atmospheric Administration (NOAA) has recently developed a new numerical method of drought detection and impact assessment from the NOAA operational environmental satellites. The method was tested during the past eight years, adjusted based on users' responses, validated against conventional data in 20 countries, including all major agricultural producers, and was accepted as a tool for the diagnosis of grain production. Now, drought can be detected 4–6 weeks earlier than before, outlined more accurately, and the impact on grain reduction can be predicted long in advance of harvest, which is most vital for global food security and trade. This paper addresses all these issues and also discusses ENSO impacts on agriculture.

1. Introduction

The main goal of global agriculture is to feed 6 billion people; a number likely to double by 2050. Grain is the principal branch that provides food and feed, making it a strategic commodity similar to energy and precious metals.

The amount of grain produced annually in a region depends on environmental resources, applied technology, and weather. The environment, including climate, ecosystems, soils, and topography, produces long-term impacts and determines a level of grain production in a region. Technology (fertilizers, pest and disease control, hybridization, melioration, mechanization, etc.) controls the long-term rate and is currently the main source of steady grain increase. Unlike technological and environmental factors, weather regulates variations in annual grain production (short term) and frequent droughts conflict with enormous technological efforts and spending in satisfying the growing world demand for food and feed.

In the past several decades, weather vagaries have caused grain shortfalls regionally and globally. Even in the last 10 years of the twentieth century [declared by the United Nations as the International Decade for Natural Disaster Reduction; Castells (1991)], widespread intensive droughts have caused huge grain shortfalls that resulted in famine, human suffering, death, abandonment of whole geographic regions, and huge economic losses in developing countries. In developed countries, the economic effect can be staggering as well (Riebsame et al. 1990; Obasi 1994; Changnon 1999). This paper describes the new operational space technology available to detect drought early enough in order to mitigate its consequences and to assess grain production well in advance of harvest, which is vital for global food security and trade. It also discusses application of the new technology for assessment of vegetation sensitivity to ENSO events.

Corresponding author address: Dr. Felix N. Kogan, NOAA/NESDIS, NOAA Science Center, 5200 Auth Road, Camp Springs, MD 20746.
E-mail: fkogan@orbit.nesdis.noaa.gov
In final form 1 February 2001.

2. Grain, technology, climate, and weather

Since grain production is so vital, how secure is it? In the last 40 years, the Green Revolution doubled the total world annual production of all types of grain from one to two billion metric tons (Fig. 1a). This success was due to development and application of new and improved technologies (fertilizers, hybridization, soil improvements, machinery, etc.). This intensive grain production increase is very important because most productive land has already been in operation and the prospects for area expansion, as seen in Fig. 1a, are slim.

Despite a steady increase in grain production, a progressively growing world demand for grain resulted in a gradual depletion of grain reserves (Fig. 1b). This means that as time goes by, less and less grain is available as an emergency supply to feed the population and domestic animals. Assuming that in one year the global harvest fails completely, wheat reserves would have been sufficient to feed the world for 5 months in the 1960s and 2.5 months at the present time. For rice, a staple food for half of the world population, and for coarse grains (barley, oats) the current reserves would last for only 1 month.

The downhill trend in reserves is aggravated by two phenomena: stagnation in the rate of the technology-related grain production increase and drought-related shortfalls (Fig. 1c). The stagnation was first observed in the mid-1970s in the United Soviet Socialist Republics (USSR) and was confirmed with a progressive intensification globally (Kogan 1986). This trend is explained by the climate constraints on technology-forced grain increase. A sluggish rate in global grain production growth is especially noticeable in the past 15 years (Fig. 1c), when frequent and large-scale intensive droughts (Kogan 1995, 1997, 2000a) claimed between 50 and 150 million tons of grain, further reducing annual reserves by up to 35%.

3. Drought as a natural disaster

Drought is a part of the earth's climate, and occurs every year without recognizing borders or economic and political differences, seriously affecting the environment, industries, and reduces agricultural production. Of all natural disasters, drought affects the largest number of people. According to the United Nations' World Meteorological Organization (Obasi 1994), between 1967 and 1991, drought affected 51% of 2.8 billion people who suffered from all natural disasters. Moreover, drought accounts for 38% of the 3.5 million people who perished (Table 1).

Drought has very unique features. Unlike other natural disasters, it starts unnoticeably and develops cumulatively, and the impact on vegetation is cumulative and not immediately observable by eye or ground data. By the time the damage is evident, it is generally too late to mitigate drought consequences (Wilhite 2000). Drought is the only natural disaster that affects all major crop and pasturelands of the world (Kogan 1997). In addition, the absence of a universal and precise drought criteria makes it difficult to detect drought early enough, estimate agricultural losses, and compare drought intensity in different ecosystems.

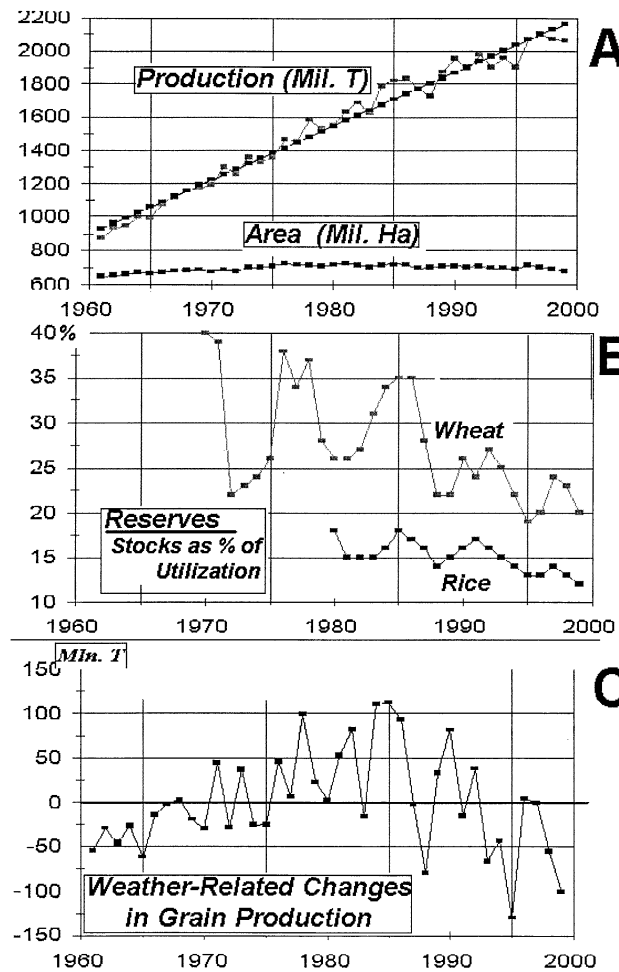

FIG. 1. World grain resources (Harnahan et al. 1984; USDA 1999; FAO 2000).

4. Operational weather satellites

Operational weather satellite measurements are good at coping with these problems. It is a paradox that weather satellites, first launched 40 years ago [1 April 1960; Rao et al. (1990)], were designed to help weather forecasters, but were found to be useful for managing vegetation distribution (Tarpley et al. 1984; Justice et al. 1985; Tucker and Sellers 1986; Townshend and Justice 1986). Since the late 1980s, they have also been used for drought detection, monitoring, and assessment of the impact on agriculture (Kogan 1990, 1995, 1997, 2000a; Hayes and Decker 1996; Liu and Kogan 1996; Unganai and Kogan 1998).

Radiances measured by the weather satellite sensors, especially by the Advanced Very High Resolution Radiometer (AVHRR) on National Oceanic and Atmospheric Administration (NOAA) polar-orbiting satellites, respond to changes in leaf chlorophyll, moisture content, and thermal conditions (Gates 1970; Myers 1970; Tucker and Sellers 1986; Gitelson and Merzlyak 1997). Over the last 20 years, the AVHRR sensor has became a "workhorse" continuously monitoring earth surface changes and is the most widely used around the world. Over the years of AVHRR sensor operation, scientists determined how best to combine AVHRR-based spectral radiances into indices and use them as proxies for estimation of the entire spectrum of vegetation health (condition) from excellent to stressed.

Moreover, AVHRR-based multiyear daily observations from space provide cost effectiveness, free access, and a repetitive view of nearly all of the earth's surfaces. They are an indispensable source of information versus in situ data whose measurements and delivery are affected by telecommunication problems and by limited access to environmentally marginal areas, places of economic disturbances, and regions of political and military conflicts. Furthermore, they are advantageous to in situ data in spatial and temporal coverage and in quick provision of data. Finally, they characterize an area rather than a point location, which is typical for agricultural and weather observations.

5. New method and data

A new method for early drought detection, monitoring, and impact assessment is based on estimation of vegetation stress from AVHRR-derived indices, designed to monitor vegetation health, moisture, and thermal conditions (Kogan 1990, 1997). Unlike the two spectral channel approach routinely applied to vegetation monitoring, the new numerical method introduced in the late 1980s is based on the combination of three spectral channels: visible (VIS), near-infrared (NIR), and 10.3–11.3-μm infrared (IR, ch4). Moreover, versus other approaches, the new method is built on three basic environmental laws: law of minimum (LOM), law of tolerance (LOT), and the principle of carrying capacity (CC).

The Leibig's LOM postulates that primary production is proportional to the amount of the most limiting growth resource and becomes the lowest when one of the factors is at the extreme minimum. Shelford's LOT states that each environmental factor that an organism or ecosystem depends upon has maximum and minimum limiting effects wherein lies a range that is called the limits of tolerance. With regard to these laws, the CC is defined as the maximal population size of a given species that the resources of a habitat can support (Ehrlich and Holdren 1971; Holdren and Ehrlich 1974; Reinign 1974; Hardin 1986; Orians 1990).

The new method was applied to the NOAA Global Vegetation Index (GVI) dataset issued routinely since 1985 (Kidwell 1997). The GVI is produced by sampling the AVHRR-based 4-km (global area coverage format) daily radiances in the VIS (0.58–0.68 μm), NIR (0.72–1.1 μm), and IR (10.3–11.3 μm and 11.5–

TABLE 1. World population affected and killed by natural disasters during 1967-91 (Obasi 1994). Total number: affected, 2.8 billion; killed, 3.5 million.

Disaster type	Affected (%)	Killed (%)
Weather		
Drought	50.9	38.1
Flood	37.8	8.7
Cyclone, hurricane, storm	7.8	27.1
Geological		
Earthquake	1.5	18.0
Volcano	0.1	0.1

Note: Percent is calculated from the total number.

12.5 μm), which were truncated to 8-bit precision and mapped to a (16 km)^2 latitude–longitude grid. To minimize cloud effects, these maps were composited over a 7-day period by saving reflectances for the day that had the largest NIR–VIS difference.

Since AVHRR-based radiances have both interannual and intraannual noise (variable illumination and viewing conditions, sensor degradation, satellite navigation and orbital drift, atmospheric and surface conditions, methods of data sampling and processing, communication and random errors), its removal is crucial for data use. The initial processing included postlaunch calibration of VIS and NIR (Rao and Chen 1995, 1999), calculation of normalized difference vegetation index [NDVI = (NIR − VIS)/(NIR + VIS)], and converting the ch4 radiance to brightness temperature (BT), which was corrected for nonlinear behavior of the sensor (Weinreb et al. 1990; Kidwell 1997).

The three-channel algorithm consists of comprehensive processing of NDVI and BT, which includes the complete removal of temporal high-frequency noise, stratification of world ecosystems, and detection of medium-to-low-frequency fluctuations in vegetation condition associated with weather variations (Kogan 1995, 1997). These steps are crucial in order to use AVHRR-based indices as a proxy for temporal and spatial analysis and interpretation of weather-related vegetation condition and health.

Three indices characterizing moisture (VCI), thermal (TCI), and vegetation health (VT) conditions were constructed from the processed (calibrated and smoothed over time) NDVI and BT following the principle of comparing a particular year NDVI and BT with the range of their variation during the extreme (stressed to favorable) conditions. Based on the LOM, LOT, and CC, the extreme conditions were derived by calculating the maximum and minimum (MAX–MIN) NDVI and BT values from 14-yr of satellite data for each land pixel (nearly 700 000). The (MAX–MIN) criteria were used to describe and classify weather-related ecosystems' "carrying capacity." The VCI, TCI, and VTI were formalized as

$$\mathrm{VCI} = (\mathrm{NDVI} - \mathrm{NDVI}_{\min})/(\mathrm{NDVI}_{\max} - \mathrm{NDVI}_{\min})100, \quad (1)$$

$$\mathrm{TCI} = (\mathrm{BT}_{\max} - \mathrm{BT})/(\mathrm{BT}_{\max} - \mathrm{BT}_{\min})100, \text{ and} \quad (2)$$

$$\mathrm{VTI} = a(\mathrm{VCI}) + b(\mathrm{TCI}), \quad (3)$$

where NDVI, $\mathrm{NDVI}_{\max}$, and $\mathrm{NDVI}_{\min}$ are the smoothed weekly NDVI, its multiyear absolute maximum, and its minimum, respectively; BT, $\mathrm{BT}_{\max}$, and $\mathrm{BT}_{\min}$ are similar values for brightness temperature; and a and b are coefficients quantifying a share of VCI and TCI contribution in the combined condition. For example, if other conditions are near normal, vegetation is more sensitive to moisture during canopy formation (leaf appearance) and to temperature during flowering. Therefore, the share of moisture contribution into the total vegetation condition (health) is higher than temperature during leaf canopy formation and lower during flowering. Since moisture and temperature contribution during a vegetation cycle is currently not known, we assume that the share of weekly VCI and TCI is equal.

Figure 2 demonstrates the above-mentioned ideas. For a selected area in Kazakhstan, NDVI and BT, for dry 1996 and wet 1997, contributed mainly to the derivation of the MAX–MIN envelope during the course of the year (Fig. 2a). An exception was some period in early spring (weeks 10–20) and late fall (BT only, weeks 35–40), when data from other years were selected to represent the extreme range. Figure 2b illustrates how the NDVI- and BT-based vegetation conditions were estimated relative to the MAX–MIN interval shown in Fig. 2a. If NDVI and BT values for a particular week are halfway between the MAX and MIN, VCI- and TCI-based vegetation conditions are estimated at the average level (around 50, Fig. 2b, weeks 14–18 for VCI and weeks 15 and 38 for TCI); if NDVI is close to the MIN and BT to the MAX, conditions are stressed (1996, Fig. 2b). Conditions are favorable if the reverse occurs (growing season of 1997, Fig. 2b). Finally, VTI in Fig. 2c estimates total vegetation health from VCI and TCI conditions. If conditions are favorable (VCI, TCI, and VT are larger than 70), vegetation is healthy; in an opposite combination, vegetation is stressed (VTI below 40). Extremely unhealthy vegetation conditions (low VTI) are normally associated with both severe moisture (VCI) and thermal (TCI) stress (1996 in Fig. 2), while favorable moisture/thermal conditions characterize healthy vegetation (high VCI, TCI, and VTI in 1997, Fig. 2). The 1996 and 1997 data represent only two of the many possible combinations of VCI- and TCI-based vegetation and temperature conditions.

6. Major world droughts and vegetation stress

Major world droughts produce staggering economic, social, and physical impacts resulting in water supply shortages, destruction of ecological

resources, and agricultural losses. The latter leads to famine and death in the developing countries and significant economic problems in the developed countries, which lead to serious consequences for the world economy. A few cases from the past 15 years are discussed below.

a. United States

The United States is the world's second largest grain producer (11%, China 20%) and the leading grain exporter. In the global grain market, the country provides up to 70% of the corn, nearly 50% of the coarse grains, and 30% of the wheat (FAO 2000) Thus, U.S. grain production is crucial both for the domestic budget and the world economy.

Drought is typical for the North American climate and occurs almost every year. Nearly 80% of the United States is located in the climatic zone where the annual consumption of water by plants exceeds precipitation (Gol'tsberg 1972, 21–22). Over the past century, many major U.S. droughts and dry spells have had significant economic, social, and environmental impacts. The famous drought of the 1930s dust bowl period affected the American economy for several years (Wilhite 2000).

A classic example of devastation is the 1988 drought, which cost around $40 billion in damage to the U.S. economy in human health, environment, and wildlife (compared to $15 billion for the 1989 San Francisco earthquake). The 1988 drought ranks as one of the nation's greatest disasters of the twentieth century. Yields of agricultural crops dropped so sharply that grain production fell below domestic consumption, probably for the first time in the last half a century (Riebsame et al. 1990; Kogan 1995; Wilhite 2000).

The AVHRR-based estimate in Fig. 3 shows that by the end of June 1988, vegetation was stressed in the most productive areas of the Great Plains, the U.S. grain basket, and the Midwest, the U.S. corn belt. The effect of the drought was exacerbated by the time of its occurrence (during a critical period of crop growth) and the worst combination of intensive VCI and TCI stress. Total U.S. corn and spring wheat production dropped by nearly 30% and 40% (USDA 2001), respectively, and the most affected states were in the zone of severe vegetation stress triggered by a 3-month-long shortage of rain (Kogan 1995). The economic effect of this drought was felt globally because the 1988 total world corn production was 50 million tons less than in 1987 and 75 million tons less than in 1989. Total world grain in 1988 dropped 3% (FAO 2000).

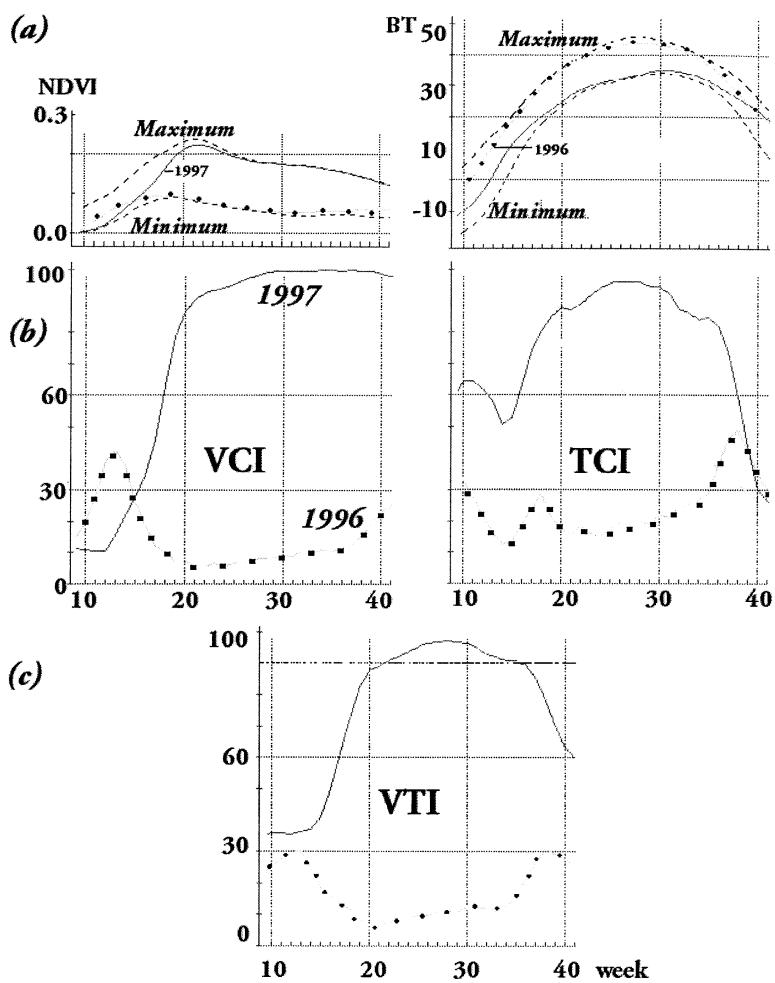

FIG. 2. Explanation of the major steps in the algorithm development; Kazakhstan (47°–48°N, 50°–51°E): (a) MAX–MIN time series (dashed) as an indicator of ecosystem "carrying capacity" and 1996 (dry) and 1997 (wet)—left, NDVI; right, BT (°C); (b) VCI and TCI time series showing extreme conditions—stressed in 1996 and favorable in 1997; and (c) vegetation health (VTI) showing healthy conditions in 1997 and unhealthy conditions in 1996.

Other major U.S. droughts of the last 15 years included 1989 and 1996, which were quite similar. Both started very early and, by the end of March, affected the primary winter wheat areas (Fig. 4, left panel); total U.S. winter wheat production dropped nearly 12% (USDA 2001). Compared with these two years, the 1988 vegetation stress at the end of March was much less intensive (light red shade) and was localized in

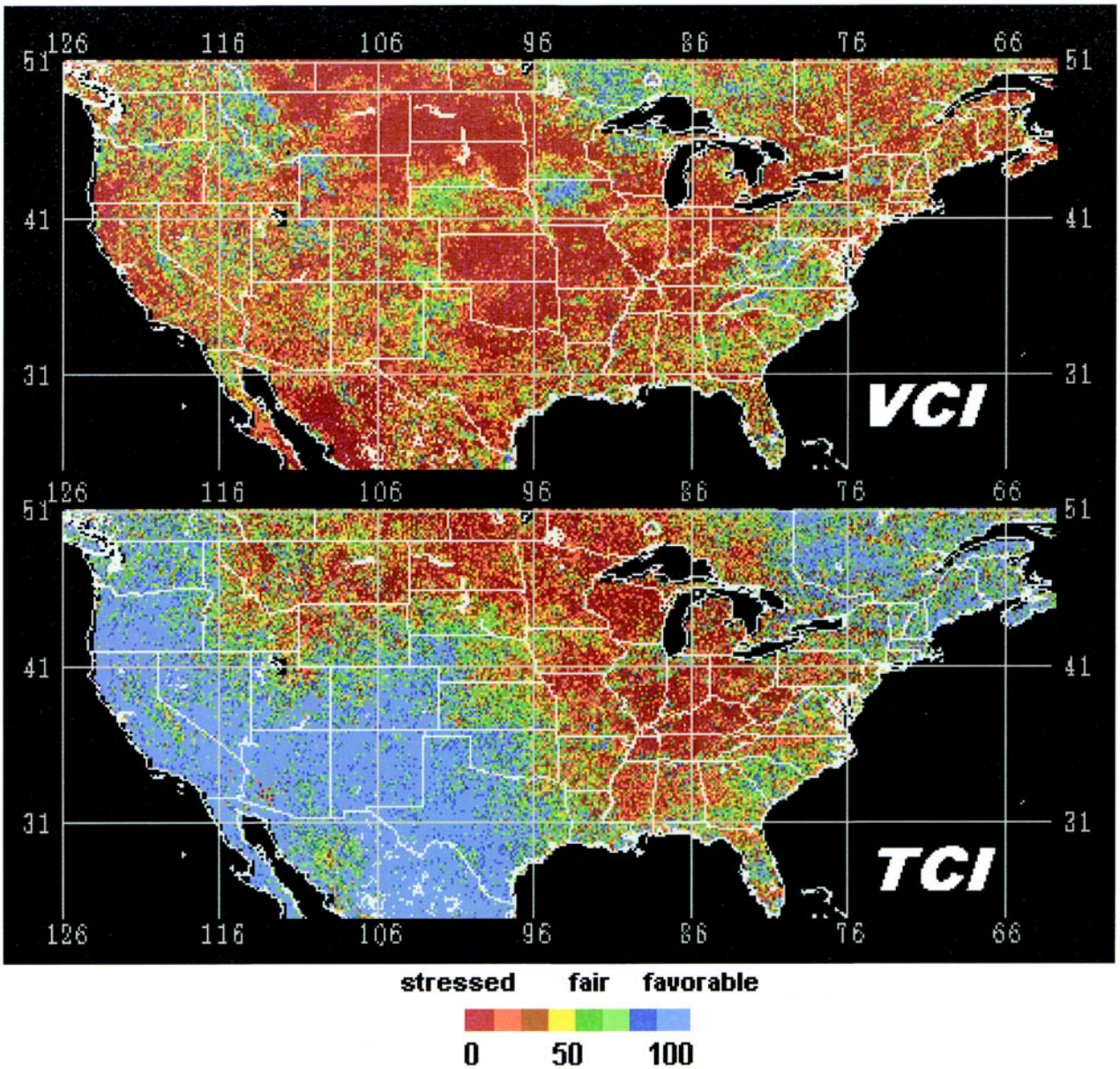

FIG. 3. VCI and TCI conditions at the end of Jun 1988 in the United States (red shade indicates drought-related vegetation stress).

the southern states only. Meanwhile, three months later, the 1988 drought turned into a national disaster, affecting vegetation during the most critical midseason period (Fig. 4, right panel). The 1989 and 1996 vegetation stresses were continuing to persist in the areas, but were not as widespread as in 1988. In 1989, the drought intensified to the north affecting the spring wheat in a few states of the central and northern Great Plains; the 1996 drought, in addition to Texas, affected grasslands of the western states. Overall, the total U.S. spring crop production in 1989 and 1996 did not shrink much and was near and slightly below normal (USDA 2001).

Because satellite-measured radiances reflect subtle changes in the vegetation canopy, they are advantageous to in situ data for early drought detection. For example, early signs of the 1988 vegetation stress in the southern United States were recorded in late March by VTI estimates (red to yellow shade), while ground estimates indicated drought several weeks later (NOAA 1988; Kogan 1995). In some years, a cool spring might delay vegetation green-up, which could potentially lead to low VCI values and misinterpretation of drought conditions (a similar situation might occur in the fall). Combining VCI and TCI into a VTI index eliminates the misrepresentation problem, as

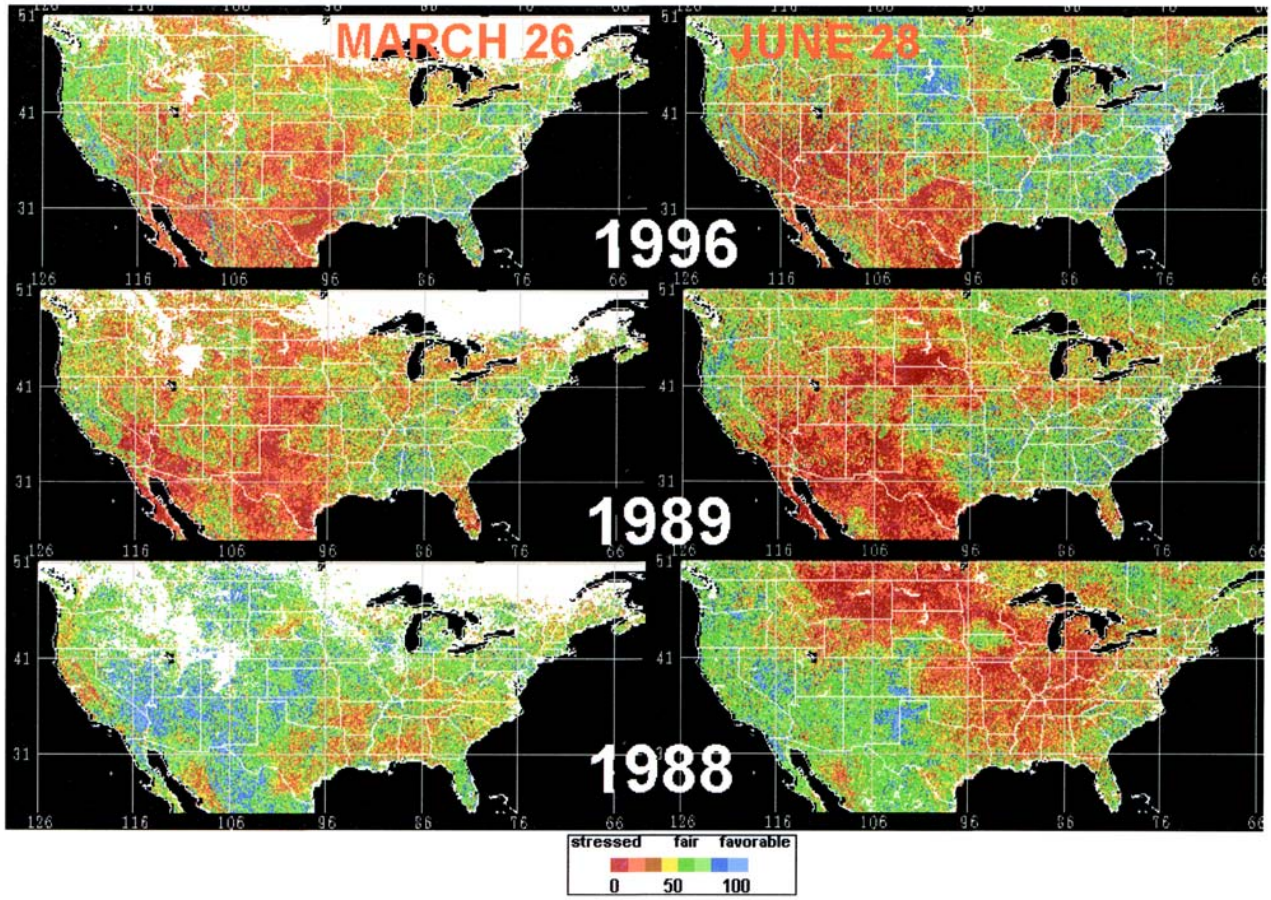

FIG. 4. Vegetation health index (VT), for the United States from *NOAA-9, -11,* and *-14* polar-orbiting satellites data; area of major U.S. droughts (1988, 1989, 1996) is outlined by vegetation stress (red shade).

high TCI values (reflecting cooler temperature conditions) offset low VCI values.

b. Former Soviet Union

If the United States is the largest seller of grain, the former Soviet Union (FSU) has been and will likely remain the largest buyer of U.S. grain. In the past 100 years, Russia has dominated the global grain market. However the paradox is that in the early twentieth century, Russia exported grain, providing more than half of the total world grain volume in trade. Seventy years later, the USSR was importing grain. In the late 1970s and during the 1980s, annual grain purchases reached an exceptionally high level, surpassing those of the entire African continent (Kogan 1985; USDA 1996). Since the USSR's breakup in 1991, agriculture of the independent states has continued to deteriorate, leading to stagnation in technology-related grain growth, which in combination with frequent drought-related shortfalls, leads to serious grain shortages in these countries. Therefore, monitoring the FSU grain production and possible purchases is very important for U.S. grain growers and traders.

The principal FSU grain regions are located in arid zones with annual precipitation deficits between 200 and 400 mm (Gol'tsberg 1972, 21–22; Kogan 1985). Climate and weather are key factors that put considerable constraints on agriculture, especially grain production. Droughts have always been the leading cause of grain shortfalls and the massive increase in grain imports (Kogan 1985). No other country in the world is as important for the global grain economy and, at the same time, extremely vulnerable to drought. Unlike other drought-prone regions, droughts in FSU are accompanied by hot and dry winds (sukhovey), which can desiccate crops in a matter of days. Moreover, droughts are frequent; catastrophic droughts occur every 8–12 years, but extreme large-area droughts hit main grain-producing regions every 2–5 years, leading to major grain shortfalls.

Since 1991, four major (including two that occurred consecutively in 1995 and 1996) and two mi-

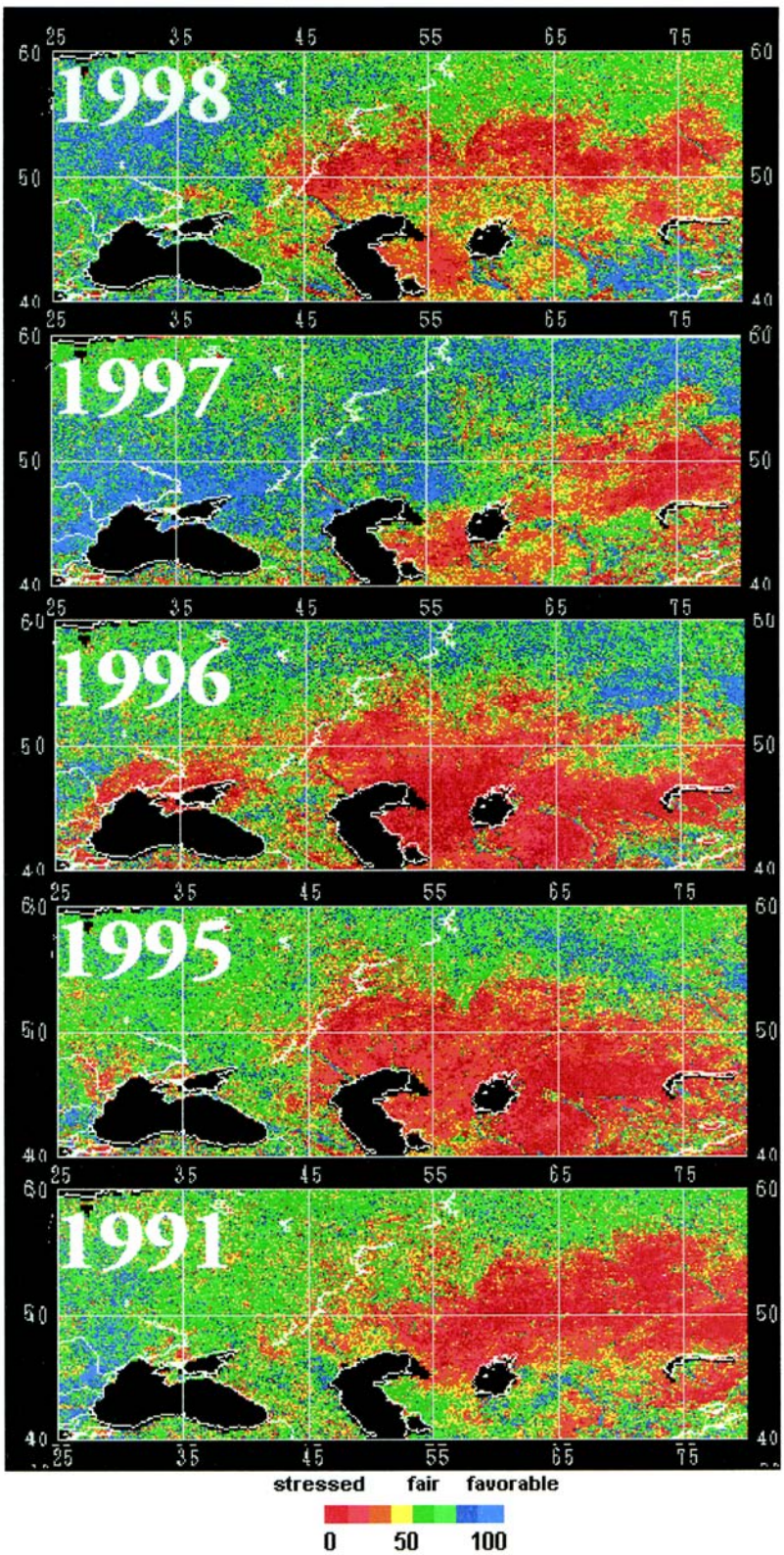

FIG. 5. The VT for FSU from *NOAA-11* and *-14* polar-orbiting satellites data; red area outlines drought-related vegetation stress.

nor droughts have been identified by the AVHRR-based indices (Fig. 5, except for the 1994 drought when satellite data were not available). These droughts covered 100–150 million acres of crops and rangeland and reduced the total FSU grain production by 10%–15% (20–30 million metric tons). The new independent countries incurred up to 30% grain loss. The worst economic problems occur when major drought affects both winter (mostly Ukraine and southern Russia) and spring grain crops (1991, 1996).

As seen in Fig. 5, FSU's droughts over the last 10 years affected mostly Kazakhstan and south-central Russia (west Siberia, Ural, and middle/lower Volga). The largest grain losses in Kazakhstan and west Siberia occurred in 1991 because vegetation was severely stressed (dark red shade) in the principal areas of spring wheat cultivation (around 50°N parallel). A fairly similar situation occurred in 1998 when wheat losses (relative to the average grain production during 1992–99) reached 30% in Russia and 40% in Kazakhstan (FAO 2000). The most productive spring wheat areas in Russia, such as the middle and lower Volga (north of the Caspian Sea), also suffered from severe vegetation stress in 1995 and 1996. These two droughts spread over the largest area; in Kazakhstan, in addition to crop damage, they severely affected rangelands (east of the Caspian Sea), which provide feed to large herds of sheep that graze all year round. Another FSU grain basket is Ukraine. Summer crops (mainly barley and corn) in that region were stressed severely during the 1996 growing season (Fig. 5). Moreover, since the summer drought in Ukraine coincided with early spring drought, which damaged winter wheat during the reproductive stage, overall grain losses in 1996 reached 20% (FAO 2000). Of all droughts of the last decades, that of 1997 had mini-

mal effect on crops (eastern Kazakhstan only).

c. Argentina

Being the major grain seller, the United States producers and traders have to constantly evaluate and closely monitor the grain industry performance of the world's major competitors. One of them is Argentina, which is the second largest exporter (after the United States) of corn and coarse grains, and the third largest of wheat. From the principal grains traders of the 1996 and 1997 world market, Argentina provided 10%–11% of wheat, 12%–15% of coarse grains, and 16%–18% of corn (FAO 2000). Droughts do not bypass Argentina since the climate provides considerably less precipitation than thermal resources can potentially evaporate, and droughts and dry spells are frequent and devastating (Gol'tsberg 1972, 21–22; Kogan 1997).

In the last 15 years, Argentina experienced two major and several minor droughts. By all standards, the most damaging droughts occurred during the 1988/89 and 1989/90 crop seasons (Fig. 6). Similar to the 1988 drought in the United States, they were large scale, very intensive, and covered the most productive agricultural areas during the critical time of grain formation. As a result, the country lost between 15% and 20% of the total volume of grain (Fig. 7). Meanwhile, the 1989/90 drought (Fig. 6) was not as intensive and widespread, and losses of grain were 3% smaller.

The minor droughts were less intensive and affected either smaller areas or only a part of the growing season, which led to up to a 10% reduction in crop yields. One such drought occurred in 1995. It began in December 1994, and by the end of January 1995 affected (light red and yellow shades in Fig. 6)

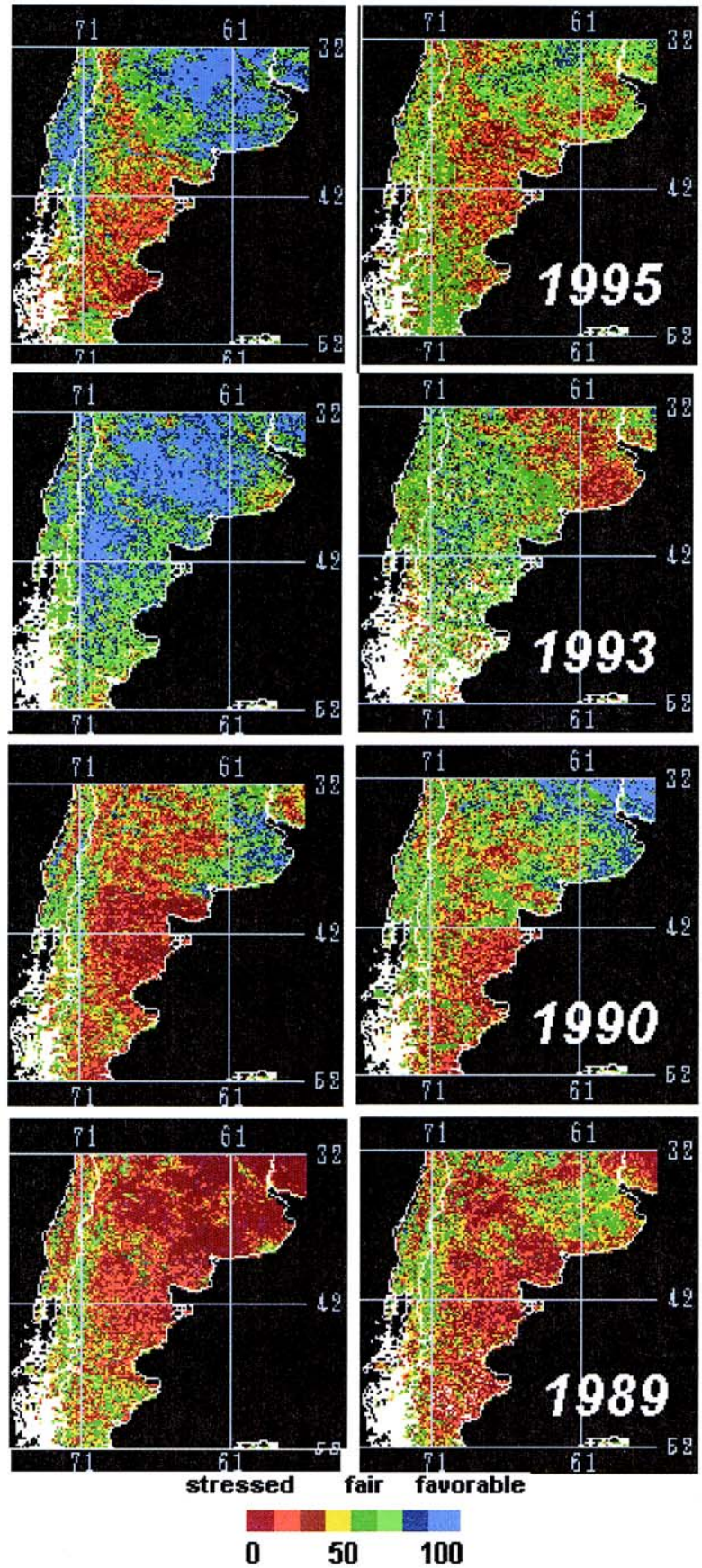

FIG. 6. The VT for Argentina from *NOAA-11* and *-14* polar-orbiting satellites data; red area outlines drought-related vegetation stress.

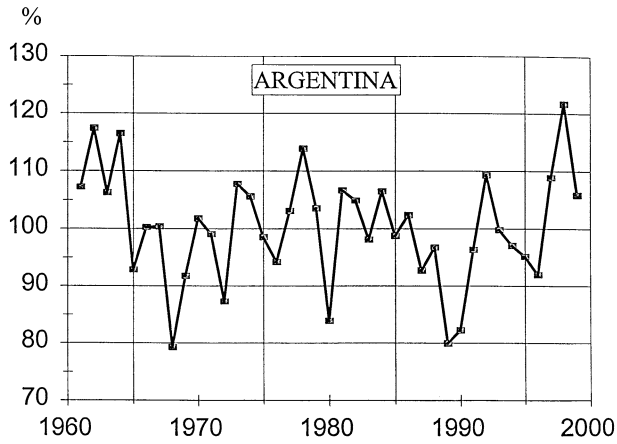

FIG. 7. Weather-related variation (percent departure from technological trend) in wheat yield during 1960–99 for Argentina; reductions of more than 5% (below 100%) are associated with droughts.

La Pampa (north of 42°S), which is a minor agricultural province in Argentina. Although the drought spread slightly to the north by the end of March, it only reached the southern part of the two major grain producing provinces (Cordoba and Santa Fe) and did not intensify (light red and yellow shades remain). Following these conditions, grain production in 1995 dropped only by 5%. In 1993, another minor drought affected one of Argentina's major provinces (Buenos Aires, east of 61°W). However, wheat production in Argentina was near normal because the drought occurred only at the end of the growing season; during the critical period of wheat reproduction (30 January), vegetation conditions were favorable (blue shade).

d. China

China is the world's leading agricultural country, producing the largest portion of global grain, including a quarter of the total wheat, one-third of the rice, and one-fifth of the corn. Among other valuable crops, the largest volume of cotton is harvested in China. Being the leader in agricultural production, most is consumed domestically and normally only a small portion is exported. For example in 1997, around 7 million tons of corn were sold to Africa (FAO 2000).

From time to time, China also imports small amounts of agricultural commodities. However, in 1994, China unexpectedly purchased a huge volume of cotton, exceeding by almost twofold the largest purchases since 1981. These imports were preceded by a cotton yield reduction three years in a row: 22% in 1992/93, 11% in 1993/94, and 7% in 1994/95 [the estimates were relative to the average yield in the very productive 1990/91 and 1991/92 seasons; USDA (1994)]. Our investigation indicates that this reduction can be attributed to unfavorable growing conditions, which caused vegetation stress in the main cotton-growing areas (Fig. 8). Of all three years, the most severe vegetation stress (both moisture and thermal) was in 1992, which also showed the largest yield reduction. Some deterioration of vegetation conditions was also observed in 1994 but the drought-related stress was partially offset by a near-normal summer rainfall. Unlike the two drought years,1993 AVHRR-derived vegetation stress in the cotton-growing area was due to excessive moisture (Kogan 1997).

7. ENSO and vegetation health around the world

The recent (1997/98) strong El Niño and the subsequent 2-yr La Niña disturbed weather and land ecosystems worldwide. They affected agriculture, fisheries, transportation, tourism, energy consumption, human health, environment, and water resources in many countries with total societal impact estimated in billions of dollars (Changnon 1999; Pielke and Landsea 1999). El Niño and La Niña (elements of ENSO) are two parts of a multiyear cycle triggered by the coupled ocean–atmosphere interaction in the tropical Pacific. They are characterized by the emergence of a huge mass of warm (El Niño) and cool (La Niña) water in the central and eastern tropical Pacific (WMO 1995; Trenberth 1997).

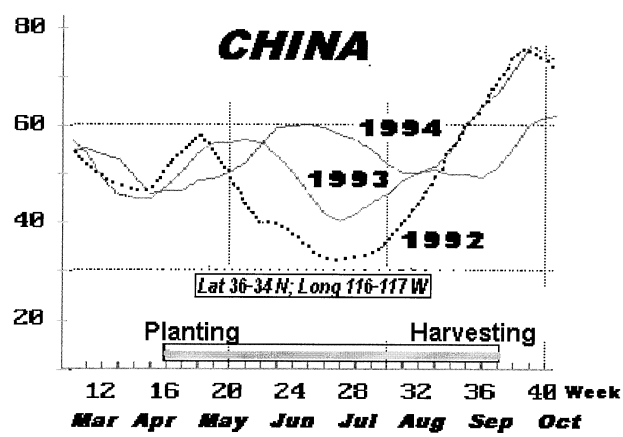

FIG. 8. Vegetation health dynamics in Shandong Province (which provides 25% of China's total cotton production) during the cotton growing season; the strongest and longest vegetation stress (VT below 40) was in 1992.

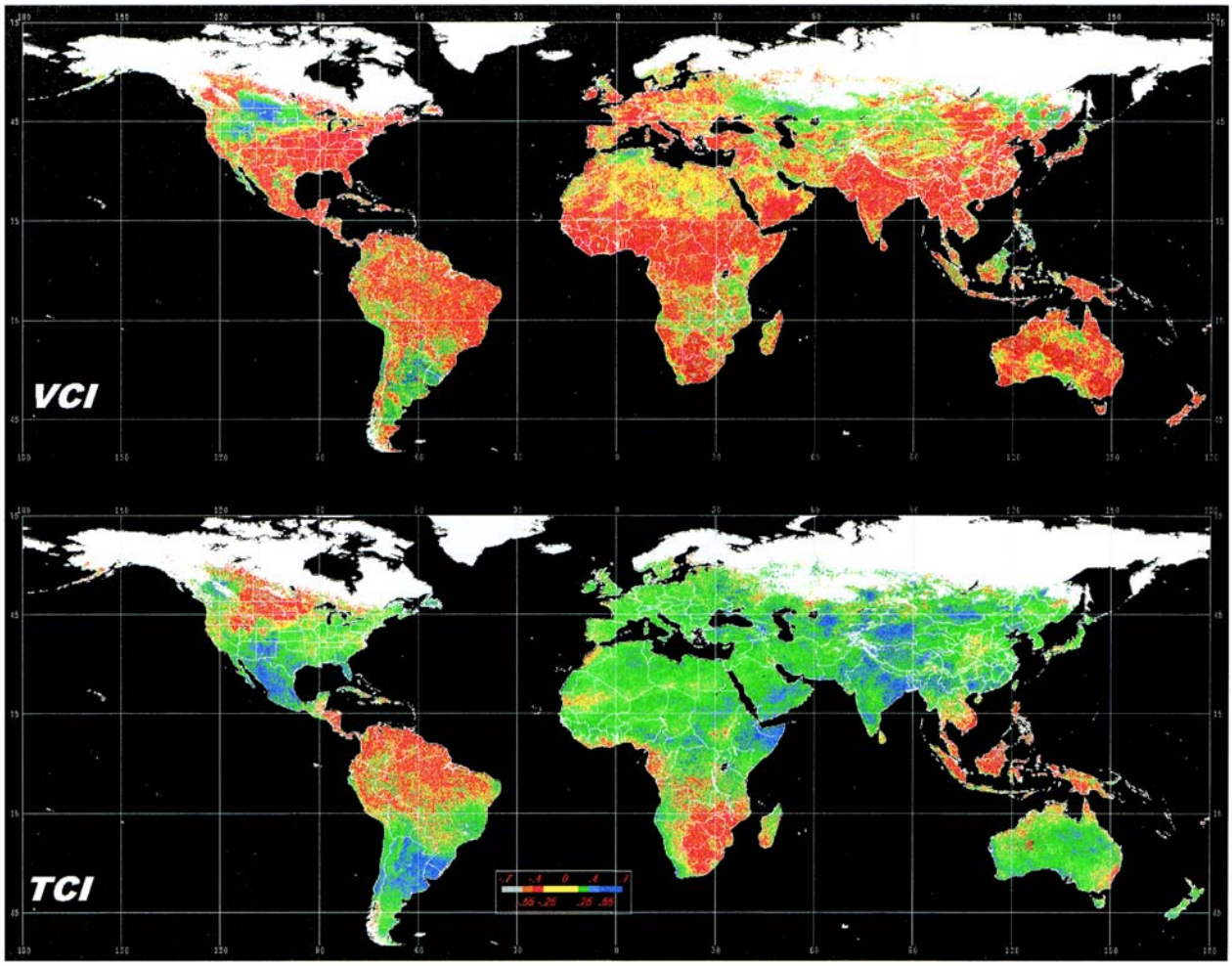

FIG. 9. Color-coded maps of correlation coefficients (R) between monthly average (calculated from weekly values) VCI and TCI with monthly SST anomaly (Niño-3.4 area) for boreal winter (Dec–Feb) 1985-1997. Color legend: yellow, $-0.25 < R < 0.25$; red/green, $|0.25| < R < |0.41|$; brown/light blue, $|0.4| < R < |0.55|$; gray/dark blue, $-R > |0.55|$. The Rs were calculated for 137 pairs of observations and are significant at 1% when $R >= |0.25$. Interpretation of VCI–SST and TCI–SST correlations: positive correlation (green/blue), below normal SST (La Niña) is associated with vegetation stress (VCI or TCI is below 35), and above normal SST indicates favorable conditions (VCI or TCI is larger than 70); negative correlation healthy and unhealthy vegetation conditions are associated with below (La Niña) and above (El Niño) normal SST, respectively.

Important ENSO implications for land ecosystems are droughts in some areas and plentiful rains in others. Conventional data show that the ENSO signal is more pronounced during boreal winter and that certain areas are more vulnerable then others (Ropelewski and Halpert 1987, 1989, 1996; Trenberth 1997). For example, Southeast Asia, southern Africa, and northern Brazil experience dry and hot weather in El Niño (warm phase) years versus wet and cool weather in La Niña (cool phase) years; central South America has an opposite response. Since these results were obtained from spatially limited weather data, the AVHRR-based indices of environmental conditions were used to outline more accurately the area of ENSO impacts (Kogan 1998, 2000b).

Figure 9 shows VCI and TCI spatial sensitivity of land ecosystems to ENSO during boreal winter (Dec–Feb). These two color-coded maps were obtained by correlating VCI and TCI (pixel by pixel) for December, January, and February with the corresponding month's sea surface temperature (SST) anomalies in the tropical Pacific (Niño-3.4 area, from 5°N to 5°S and from 120° to 170°W). The period of correlation was from 1985 through 1997, excluding December 1994 and January 1995 when the *NOAA-11* satellite was inoperative. The VCI–SST and TCI–SST correlation coefficients (R) range from –0.55 to 0.54. Since 1% of significance is reached for $R \geq |0.25|$, this range is further discussed and the yellow area on the map is considered as the background where the correlation is

TABLE 2. Correlation matrix of mean regional spring wheat yield (deviation from technological trend) vs mean regional VCI and TCI for Kazakhstan (Kokchetav oblast), 1985–97.

Week	VCI	TCI
24	0.0	0.71
25	0.24	0.76
26	0.48	0.80
27	0.64	0.76
28	0.77	0.71
29	0.83	0.66
30	0.86	0.63
31	0.84	0.57
32	0.79	0.58
33	0.70	0.61
34	0.59	0.67

negligible. Even if the correlation is above |0.25|, for the majority of the world pixels in Fig. 9, the correlation is low. Therefore, a higher sensitivity of vegetation in a given region to SST should be considered relative to a lower sensitivity in other regions. Regarding an interpretation of SST impacts on ecosystems, a general rule is, in the areas of positive correlation (green-blue shade), below normal SST (La Niña) is associated with vegetation stress (VCI or TCI below 30) while above normal SST (El Niño) results in favorable conditions (indices above 70). On the other hand, in the areas of negative correlation (red-brown shade), healthy/unhealthy vegetation conditions are associated with below/above (La Niña/El Niño) normal SST, respectively.

The maps in Fig. 9 show generally two types of ENSO links with VCI and TCI conditions. The first is for the same direction of the impact, when *R* for both VCI and TCI is either positive or negative. If *R* is negative (red-brown shade), then El Niño is accompanied by both VCI and TCI stress (due to drier and warmer weather), while La Niña is followed by favorable conditions. This type is typical for South Africa, South America, and most of the islands in Southeast Asia. Central South America is the only world region where both VCI–SST and TCI–SST have positive correlation (green-blue shade), which means that vegetation is healthy in El Niño and stressed in La Niña years. These results match well with ground observations (Ropelewski and Halpert 1987, 1989, 1996; Trenberth 1997; Kogan 2000b).

The second type of ENSO association with moisture and thermal land conditions occurred when VCI–SST has positive and TCI–SST negative correlation and vice versa (e.g., moisture stress but no thermal stress due to cooler temperature). The United States is one of the interesting examples in Fig. 9, which shows that in the southeastern part of the country, El Niño is associated with poorer vegetation (negative *R* in the VCI map, red-brown shade) but no association is found with thermal conditions (low *R* in the TCI map, green shade, except FL). Southwestern

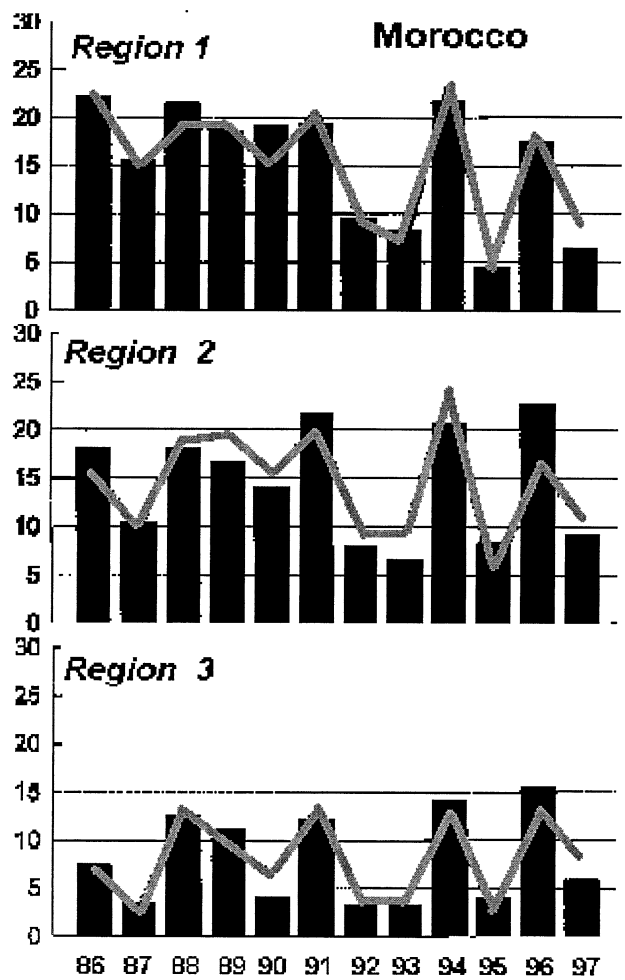

FIG. 10. Independent evaluation of wheat yield estimates from satellite (line) and ground (bars) data for Morocco, 1985–98.

states, centered around New Mexico, also experience poorer vegetation conditions (negative *R*) but at the background of strong influence of colder temperature (positive *R,* blue shade). In the northern United States and the neighboring Canadian regions, the situation is just the opposite; El Niño is associated with favorable moisture conditions (positive *R,* green-blue shade) and warmer temperatures (negative *R,* red-brown shade). Among other large world regions, central Africa, India, Southeast Asia, and parts of Australia are sensitive to moisture conditions (negative VCI–SST correlation, red-brown shade) but less sensitivity to thermal conditions (positive *R,* green-blue shade).

Satellite-based estimates of ENSO–land surface (vegetation) associations are generally in agreement with in situ observations (precipitation and temperature). However, there are a few disagreements. While satellite data show some enhanced El Niño/La Niña signal over land in central America, ground data do not. The area of the impacts in South America from ground data is smaller (only northern Brazil), while from satellite data enhanced ecosystems sensitivity is identified for the entire northern part. In central Argentina, there is a ground signal for only warm episodes (El Niño), while satellite data show vegetation response to both episodes. In the southeastern United States, El Niño/La Niña-type weather is wet/dry from ground data, which does not match the observed unhealthy/healthy vegetation conditions, respectively (Ropelewski and Halpert 1987, 1989, 1996; Trenberth 1997; Kogan 2000b). These disagreements require further investigation, which is beyond the discussion of this paper.

8. AVHRR-based crop yield prediction

Crop yield modeling has been a very successful program, specifically in areas with limited ground data.

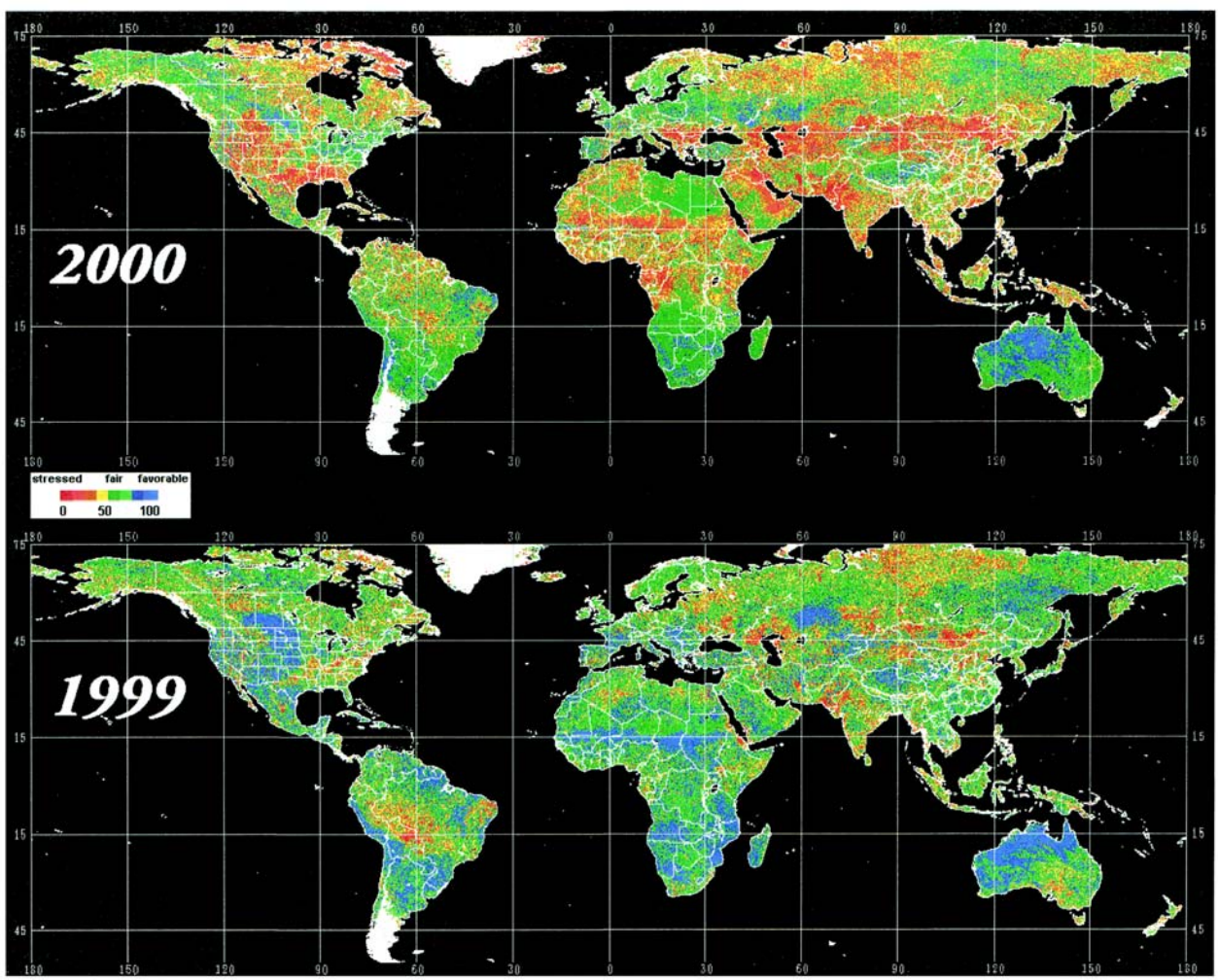

FIG. 11. Vegetation health 2000 vs 1999.

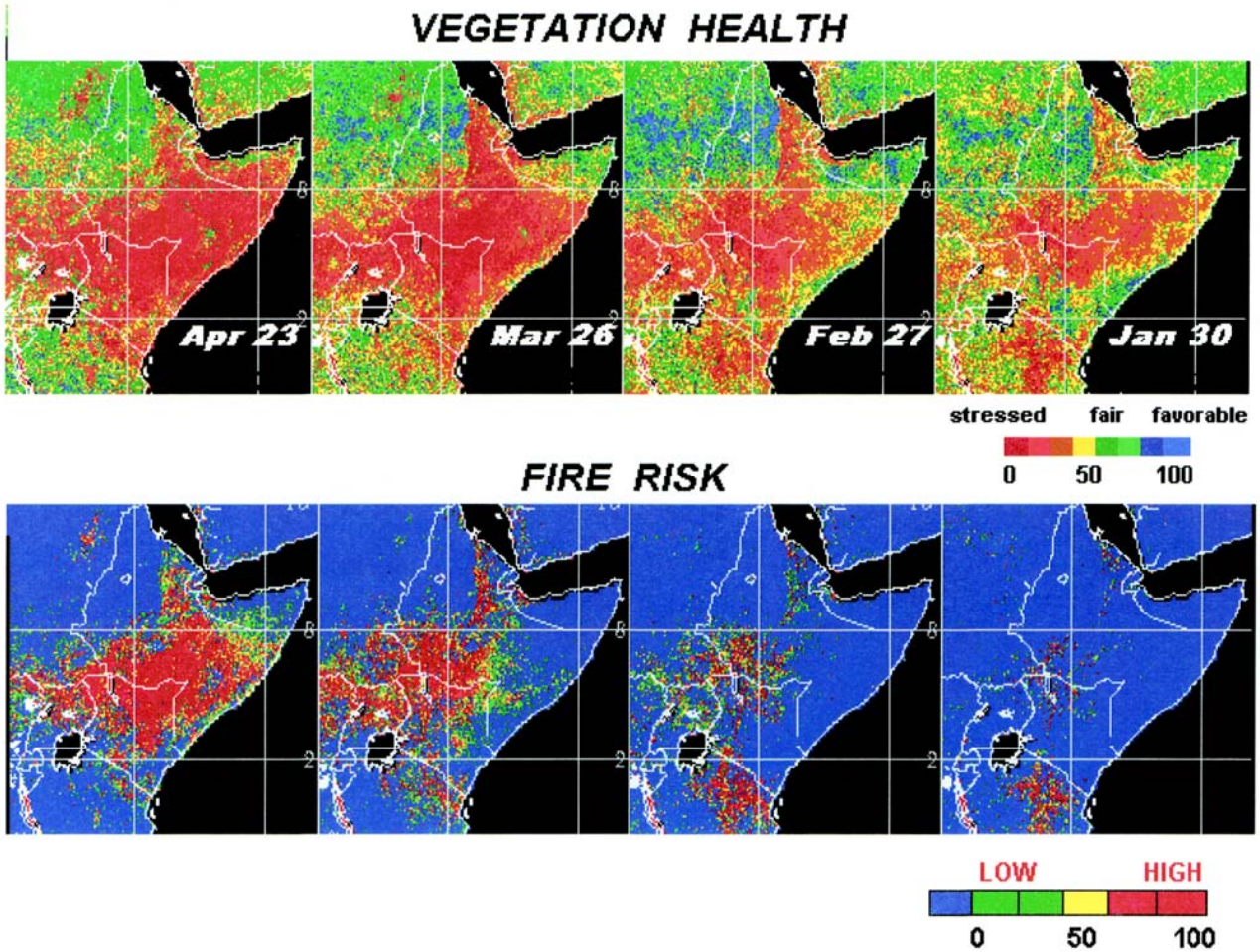

FIG. 12. Vegetation health and fire risk dynamics in the Horn of Africa, 2000.

The background for this task was laid down in the mid-1990s and was confirmed in the U.S. midwest and in Zimbabwe (Hayes and Decker 1996; Liu and Kogan 1996). It has been shown that vegetation health indices correlate highly with yield during the critical period of crop development (Table 2) and might be used for modeling and diagnosis of crop yield. Currently, satellite-based crop yield models have been developed for Argentina, Brazil, South Africa, Morocco, Poland, Hungary, Kazakhstan, India, and China. In Poland, this program was so successful that the AVHRR-based drought detection and watch method, and VCI- and TCI-based models were accepted by the government as an official tool for cereal yield diagnostics. An example of independent evaluation done in Morocco (Fig. 10) shows that regional wheat yield estimates (line) follow closely the official statistics (bar), especially in the main regions (1–3) of wheat production.

9. Vegetation health 2000

The last year of the twentieth century was marked by a new series of large area droughts in the world. Figure 11 shows midsummer 2000 vegetation health in comparison with 1999. It is evident that after a relatively favorable 1999, severe droughts covered nearly 20% of the world land affecting crops, pastureland, and forestlands in Africa, Asia, and North America (red shades). Long and intensive spring and summer droughts developed in the southern and eastern United States; in the northwestern states, the drought triggered huge forest fires. In Asia, crop-producing regions of Afghanistan, Pakistan, Iran, India, and China were severely hit by spring and summer droughts. Summer dryness also affected the new countries (from the former USSR) in the Caspian Sea region.

An interesting case was sub-Sahara Africa where drought developed in early spring and seriously affected the minor agricultural season in the Horn of Africa. Vegetation stress in the area started in Janu-

ary affecting central Somalia, southern Ethiopia, northern Kenya, and Uganda (Fig. 12). In a 4-month period, the stress intensified and expanded to new areas. By the end of April, this drought turned into a natural disaster, affecting 90% of Kenya, Somalia, and Uganda and almost all agricultural lands of Ethiopia. The minor ("belg") crop season during March–May, which normally provides food and feed before the start of the main growing season, almost completely failed. Moreover, a huge area of the entire Horn of Africa region was under the threat of fire. It was estimated that nearly 15 million people in the region were affected by this severe drought. Moreover, parts of drought-affected southwestern Somalia were suffering from cholera outbreaks as water supplies became limited and contaminated.

10. Conclusions

The results of this paper show that we begin the twenty-first century with exciting prospects for the application of operational meteorological satellites in agriculture. With the introduction of the new method, which was tested around the world, including all principal agricultural producers, drought can be detected 4–6 weeks earlier than before in any corner of the globe, outlined more accurately, and its impact on grain reduction can be diagnosed well in advance of harvest. This is a vital step for global food security and trade.

The current developments in satellite technology and sensor design, along with great achievements in numerical methods, speed, and capacity of computers, and available hardware and software, will bring more progress in the application of operational and research satellites.

With accumulation of satellite data we will continue to enhance the accuracy of hazard detection, monitor the environment, increase the lead time of estimates, and better diagnose impact assessment. New products geared toward early warning of insect development, diagnosis of epidemics, and other human health problems will be more aggressively pursued. New sensors will widen our abilities to detect problems earlier and with higher spatial accuracy. New high-resolution capabilities of satellite sensors will help with precision agriculture and the ability to move from the problem of detection to the mitigation of consequences. A new era of satellites will provide the ability to estimate the economic effectiveness of applied technologies in order to optimize profit.

Acknowledgments. The author wishes to thank NOAA for continued support; his colleagues Drs. G. Ohring, J. Tarpley, and J. Sullivan for useful discussions and advice; cooperative scientists around the world for the contribution of their data and knowledge; and my daughter, Masha Kogan, for her editorial work.

References

Castells, P. B., 1991: International Decade for Natural Disaster Reduction. *Undro News,* July/August, Office of the United Nations Disaster Relief, 19–20.

Changnon, S. A., 1999: Impacts of 1997–98 El Niño-generated weather in the United States. *Bull. Amer. Meteor. Soc.,* **80**, 1819-1827.

Ehrlich, P. R., and J. P. Holdren, 1971: Impact of population growth. *Science,* **171**, 1212-1217.

FAO, cited 2000: Crop production. [Available online at http://fao.org/page/collections.]

Gates, D. M., 1970: Physical and physiological properties of plants. *Remote Sensing with Specific Reference to Agriculture and Forestry,* National Academy of Sciences, 224–252.

Gitelson, A. A., and M. N. Merzlyak, 1997: Remote estimation of chlorophyll content in higher plant leaves. *Int. J. Remote Sens.,* **18**, 2691–2697.

Gol'tsberg, I. A., Ed., 1972: *Agroclimatic Atlas of the World.* Hydrometizdat.

Hanrahan, C. E., F. S. Urban, and J. L. Deaton, 1984: Long run changes in world food supply and demand. ERS/USDA Tech. Rep., 39 pp.

Hardin, G., 1986: Cultural carrying capacity: a biological approach to human problems. *Bio. Science,* **36**, 599–606.

Hayes, M. J., and W. L. Decker, 1996: Using NOAA AVHRR data to estimate maize production in the United States corn belt. *Int. J. Remote Sens.,* **17**, 3189-3200.

Holdren, J. P., and P. R. Ehrlich, 1974: Human population and the global environment. *Amer. Sci.,* **62**, 282-292.

Justice, C. O., J. R. G. Townshend, B. N. Holben, and C. J. Tucker, 1985: Analysis of the phenology of global vegetation using meteorological satellite data. *Int. J. Remote Sens.,* **6**, 1271–1283.

Kidwell, K. B., Ed., 1997: Global vegetation index user's guide. NOAA Tech. Rep., 65 pp.

Kogan, F. N., 1985: The sun won't keep shine on Soviet agriculture. *The Wall Street Journal,* 28 August.

——, 1986: Climate constraints and trends in global grain production. *Agric. For. Meteor.,* **37**, 89–107.

—— 1990: Remote sensing of weather impacts on vegetation in non-homogeneous areas. *Int. J. Remote Sens.,* **11**, 1405–1419.

—— 1995: Droughts of the late 1980s in the United States as derived from NOAA polar orbiting satellite data. *Bull. Amer. Meteor. Soc.,* **76**, 655–668.

—— 1997: Global drought watch from space. *Bull. Amer. Meteor. Soc.,* **78**, 621–636.

—— 1998: A typical pattern of vegetation conditions in southern Africa during El Niño years detected from AVHRR data using three-channel numerical index. *Int. J. Remote Sens.,* **18**, 3689–3695.

—— 2000a: Global drought detection and impact assessment form space. *Drought: A Global Assessment,* D. A. Wilhite, Ed., Hazard and Disaster Series, Vol. 1, Routledge, 196–210.

—— 2000b: Satellite-observed sensitivity of world land ecosystems to El Niño/La Niña. *Remote Sens. Environ.,* in press.

Liu, W. T., and F. N. Kogan, 1996: Monitoring regional drought using the vegetation condition index. *Int. J. Remote Sens.,* **17**, 2761–2782.

Myers, V. I., 1970: Soil, water, and plant relations. *Remote Sensing with Specific Reference to Agriculture and Forestry,* National Academy of Sciences, 253–267.

NOAA, 1988: Drought advisory 88/12: Summary of drought conditions and impacts. NOAA Memo., 25 pp.

Obasi, G. O. P., 1994: WMO's role in the International Decade for Natural Disaster Reduction. *Bull. Amer. Meteor. Soc.,* **75**, 1655-1661.

Orians, G. H., 1990: Ecological sustainability. *Environment,* **32**, 10–15, 34-39.

Pielke, R. A., and C. N. Landsea, 1999: La Niña, El Niño, and Atlantic hurricane damages in the United States. *Bull. Amer. Meteor. Soc.,* **80**, 2027–2033.

Rao, C. R. N., and J. Chen, 1995: Inter-satellite calibration linkages for the visible and near-infrared channels of the Advanced Very High Resolution Radiometer on the NOAA-7, -9, and -11 spacecrafts. *Int. J. Remote Sens.,* **16**, 1931-1942.

——, and ——, 1999: Revised post-launch calibration of the visible and near-infrared channels of the Advanced Very High Resolution Radiometer on the NOAA-14 spacecraft. *Int. J. Remote Sens.,* **20**, 3485–3491.

Rao, P. K., S. J. Holmes, R. K. Anderson, J. S. Winston, and P. E. Lehr, Eds., 1990: *Weather Satellites: Systems, Data and Environmental Applications.* Amer. Meteor. Soc., 503 pp.

Reinign, P., 1974: The use of ERTS-1 data in carrying capacity estimates for sites in Upper Volta and Niger. *Proc. Annual Meeting of the American Anthropological Association,* Mexico City, Mexico, American Anthropological Association, 176-180.

Riebsame, W. E., S. A. Changnon, and T. R. Karl, 1990: *Drought and Natural Resource Management in the United States: Impacts and Implications of the 1987-1989 Drought.* Westview Press, 246 pp.

Ropelewski, C. F., and M. S. Halpert, 1987: Global and regional scale precipitation patterns associated with El Niño/Southern Oscillation. *Mon. Wea. Rev.,* **115**, 1606–1626.

——, and ——, 1989: Precipitation patterns associated with the high index phase of the southern oscillation. *J. Climate,* **2**, 268-284.

——, and ——, 1996: Quantifying Southern Oscillation–precipitation relationships. *J. Climate,* **9**, 1043-1059.

Tarpley, J. P., S. R. Schnieder, and R. L. Money, 1984: Global vegetation indices from the NOAA-7 Meteorological satellite. *J. Appl. Meteor.,* **23**, 491–494.

Trenberth, K. E., 1997: Short-term climate variations: Recent accomplishments and issues for future progress. *Bull. Amer. Meteor. Soc.,* **78**, 1081–1096.

Tucker, C. J., and P. J. Sellers, 1986: Satellite remote sensing of primary production. *Int. J. Remote Sens.,* **7**, 1395–1416.

Unganai, L. S., and F. N. Kogan, 1998: Drought monitoring and corn yield estimation in southern Africa from AVHRR data. *Remote Sens. Env.,* **63**, 219-232.

USDA, 1994: *USDA Agricultural Handbook,* Handbook No. 664, Major world crop areas and climatic profiles. 157–170.

——, cited 1996: Global grain market in 1996: Shades of 1972–74? *Agricultural Outlook,* 2–6 September, USDA.

——, cited 1999: Grain: World market and trade. [Available online at http://www.fas.usda.gov/grain/circular/1999.]

———, cited 2001: National agricultural statistical service. [Available online at http://www.usda.gov/nass/aggraphs/swyld.]

Weinreb, M. P., G. Hamilton, and S. Brown, 1990: Nonlinearity correction in calibration of the Advanced Very High Resolution Radiometer infrared channels. *J. Geophys. Res.,* **95**, 7381-7388.

Wilhite, D. A., 2000: Drought as a natural hazard. *Drought: A Global Assessment,* D. A. Wilhite, Ed., Hazard and Disaster Series, Vol. 1, Routledge, 3-18.

WMO, 1995: *The Global Climate System Review: Climate System Monitoring.* 150 pp.